Majorana Fermions in Equilibrium and in Driven Cold-Atom Quantum Wires

Liang Jiang,[1,2] Takuya Kitagawa,[3] Jason Alicea,[4] A. R. Akhmerov,[5] David Pekker,[2] Gil Refael,[2] J. Ignacio Cirac,[6] Eugene Demler,[3] Mikhail D. Lukin,[3] and Peter Zoller[7]

[1]*Institute for Quantum Information, California Institute of Technology, Pasadena, California 91125, USA*
[2]*Department of Physics, California Institute of Technology, Pasadena, California 91125, USA*
[3]*Department of Physics, Harvard University, Cambridge, Massachusetts 02138, USA*
[4]*Department of Physics and Astronomy, University of California, Irvine, California 92697, USA*
[5]*Instituut-Lorentz, Universiteit Leiden, P.O. Box 9506, 2300 RA Leiden, The Netherlands*
[6]*Max-Planck-Institut für Quantenoptik, Hans-Kopfermann-Strasse 1, D-85748 Garching, Germany*
[7]*Institute for Theoretical Physics, University of Innsbruck, 6020 Innsbruck, Austria*

(Received 26 February 2011; revised manuscript received 27 April 2011; published 2 June 2011)

We introduce a new approach to create and detect Majorana fermions using optically trapped 1D fermionic atoms. In our proposed setup, two internal states of the atoms couple via an optical Raman transition—simultaneously inducing an effective spin-orbit interaction and magnetic field—while a background molecular BEC cloud generates s-wave pairing for the atoms. The resulting cold-atom quantum wire supports Majorana fermions at phase boundaries between topologically trivial and nontrivial regions, as well as "Floquet Majorana fermions" when the system is periodically driven. We analyze experimental parameters, detection schemes, and various imperfections.

DOI: 10.1103/PhysRevLett.106.220402 PACS numbers: 05.30.Pr, 03.67.Lx, 03.75.Mn

Majorana fermions (MFs), unlike ordinary fermions, are their own antiparticles and are widely sought for their exotic exchange statistics and potential for topological quantum computation. Various promising proposals exist for creating MFs as quasiparticles in 2D systems, such as quantum Hall states with filling factor $5/2$ [1], p-wave superconductors [2], topological insulator-superconductor interfaces [3,4], and semiconductor heterostructures [5]. In addition, MFs can even emerge in 1D quantum wires, such as the spinless p-wave superconducting chain [6] which is effectively realized in semiconductor wire-bulk superconductor hybrid structures with spin-orbit interaction and a strong magnetic field [7,8]. Although there are many efforts to search for MFs, their unambiguous detection remains an outstanding challenge.

Significant advances in cold-atom experiments have opened up a new era of studying many-body quantum systems. Cold atoms not only sidestep the issues of disorder and decoherence which often plague solid-state systems, but also benefit from tunable microwave and optical control of the Hamiltonian. In particular, recent experiments have demonstrated synthetic magnetic fields by introducing a spatially dependent optical coupling between different internal states of the atom [9,10], which can be generalized to create non-Abelian gauge fields with careful design of optical couplings [11,12]. For example, spin-orbit interaction can be induced in an optically coupled tripod-level system to create MFs in 2D [13–15].

In this Letter, we propose to create and detect MFs using optically trapped 1D fermionic atoms. We show that an optical Raman transition with photon recoil can induce both an effective spin-orbit interaction and an effective magnetic field. Combined with s-wave pairing induced by the surrounding BEC of Feshbach molecules, the cold-atom quantum wire supports MFs at the boundaries between topologically trivial and nontrivial superconducting regions [7]. Furthermore, the unique properties of atomic systems with their complete isolation from the environment allow a realization of *Floquet* MFs when the system is periodically driven, and we find two flavors of Floquet MFs characterized by different topological charges. In contrast to the earlier 2D cold-atom MF proposals that require sophisticated optical control, like tilted optical lattices [16] or multiple laser beams [13,15], our scheme simply uses the Raman transition. Moreover, compared with the solid-state proposals [3,7], the cold-atom quantum wire offers various advantages such as tunability of parameters and, crucially, much better control over disorder and decoherence.

Theoretical model.—We consider a system of optically trapped 1D fermionic atoms inside a 3D molecular BEC (Fig. 1). The Hamiltonian for the system reads

$$H = \sum_p a_p^\dagger(\varepsilon_p + V + \delta_{\rm RF})a_p + \sum_p (B a_{p+k,\uparrow}^\dagger a_{p-k,\downarrow} + \Delta a_{p,\uparrow}^\dagger a_{-p,\downarrow}^\dagger + \text{H.c.}). \quad (1)$$

The fermionic atoms with momentum p have two relevant internal states, represented by spinor $a_p = (a_{p,\uparrow}, a_{p,\downarrow})^T$. The kinetic energy is $\varepsilon_p = \frac{p^2}{2m}$ and the optical trapping potential is V where the 1D fermionic atoms reside. As shown in Figs. 1(a) and 1(b), two laser beams Raman couple the states $a_{p-k,\downarrow}$ and $a_{p+k,\uparrow}$ with coupling strength $B = \frac{\Omega_1\Omega_2^*}{\delta_e}$, where δ_e is the optical detuning, $\Omega_{1(2)}$ are Rabi

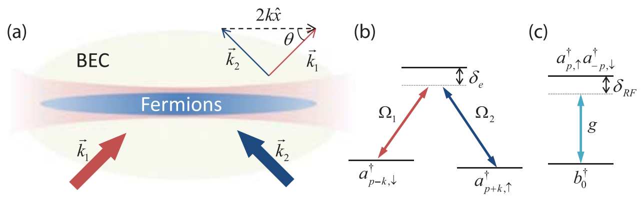

FIG. 1 (color online). (a) Optically trapped fermionic atoms form a 1D quantum wire inside a 3D molecular BEC. Two Raman beams propagate along $\vec{k}_1$ and $\vec{k}_2$ directions, respectively. The recoil momentum $\vec{k}_1 - \vec{k}_2 = 2k\hat{x}$ is parallel to the quantum wire. (b) Raman coupling between two fermionic states $a_\uparrow$ and $a_\downarrow$ induces a $2k$ momentum change from photon recoil. (c) Radio-frequency-induced atom-molecular conversion.

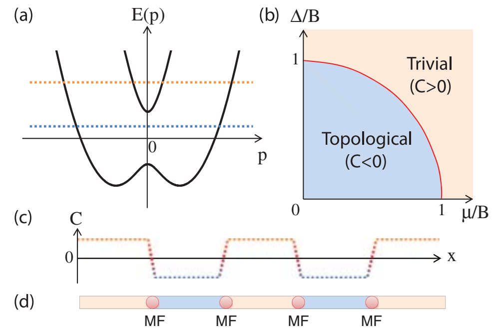

FIG. 2 (color online). (a) Energy dispersion for spin-orbit-coupled fermions in a magnetic field. There is an avoided crossing at $p = 0$ with energy splitting $2B$ (dark solid line). The horizontal dotted line represents $\sqrt{\Delta^2 + \mu^2}$, which has two crossing points when $\sqrt{\Delta^2 + \mu^2} < B$ (blue [dark gray] dotted line) and four crossing points when $\sqrt{\Delta^2 + \mu^2} > B$ (orange [light gray] dotted line). (b) Phase diagram for topological and trivial phases with respect to parameters of Δ and μ. (c), (d) $C(x)$ can take positive or negative values, which divides the quantum wire into alternating regions of topological and trivial phases.

frequencies, and $\vec{k}_1 - \vec{k}_2 = 2k\hat{x}$ is the photon recoil momentum parallel to the quantum wire. The bulk BEC consists of Feshbach molecules ($b \rightleftharpoons a_\uparrow + a_\downarrow$) [17] with macroscopic occupation in the ground state $\langle b_0 \rangle = \Xi$. The interaction between the fermionic atoms and Feshbach molecules can be induced by an rf field, which has detuning $\delta_{\rm rf}$ and Rabi frequency $g = \gamma_B A_{\rm rf}$ with magnetic dipole moment γ_B and rf field amplitude $A_{\rm rf}$. In the rotating frame associated with the rf field, the interaction between b and $a_\uparrow + a_\downarrow$ is $g b a_\uparrow^\dagger a_\downarrow^\dagger \approx \Delta a_\uparrow^\dagger a_\downarrow^\dagger$, with $\Delta \approx g\Xi$ [18].

We can recast the Hamiltonian into a more transparent form by applying a unitary operation that induces a spin-dependent Galilean transformation, $U = e^{ik\int x(a_{x,\uparrow}^\dagger a_{x,\uparrow} - a_{x,\downarrow}^\dagger a_{x,\downarrow})dx}$, where x is the coordinate along the quantum wire. Depending on the spin, the transformation changes the momentum by $\pm k$, $U a_{p+k,\uparrow} U^\dagger = a_{p,\uparrow}$ and $U a_{p-k,\downarrow} U^\dagger = a_{p,\downarrow}$. The transformed kinetic energy becomes spin-dependent $(p + k\sigma_z)^2/2m$, which consists of spin-independent part $\varepsilon_p' = p^2/2m$, spin-orbit interaction $kp\sigma_z/m$, and constant energy shift $k^2/2m$. The transformed Hamiltonian closely resembles the semiconducting wire model studied in [7] and reads

$$H = \sum_p a_p^\dagger(\varepsilon_p' - \mu + up\sigma_z + B\sigma_x)a_p + (\Delta a_{p,\uparrow}^\dagger a_{-p,\downarrow}^\dagger + \text{H.c.}), \qquad (2)$$

where $\mu \equiv -(\delta_{\rm rf} + V + \varepsilon_k)$ is the local chemical potential and the velocity $u = k/m$ determines the strength of the effective spin-orbit interaction.

Topological and trivial phases.—The physics of the quantum wire is determined by four parameters: the s-wave pairing energy Δ, the effective magnetic field B, the chemical potential μ, and the spin-orbit interaction energy $E_{\rm so} = mu^2/2$. For $p \neq 0$, the determinant of H_p' is positive definite, so the quantum wire system has an energy gap at nonzero momenta. For $p = 0$, however, H_p' yields an energy $E_0 = B - \sqrt{\Delta^2 + \mu^2}$ which vanishes when the quantity $C \equiv \Delta^2 + \mu^2 - B^2$ equals zero, signaling a phase transition [7] [see Fig. 2(b)]. When $C > 0$ the quantum wire realizes a trivial superconducting phase. For example, when $B \ll \Delta$, μ all energy gaps are dominated by the pairing term, yielding an ordinary spinful 1D superconductor. When $C < 0$ a topological superconducting state emerges. For instance, when $B \gg \Delta$, μ, $E_{\rm so}$ the physics is dominated by a single spin component with an effective p-wave pairing energy $\Delta_p \approx \Delta \frac{up}{B}$; this is essentially Kitaev's spinless p-wave superconducting chain, which is topologically nontrivial and supports MFs [6].

With spatially dependent parameters (μ, B or Δ), we can create boundaries between topological and trivial phases. MFs will emerge at these boundaries [7]. Spatial dependence of $\mu(x)$ can be generated by additional laser beams with nonuniform optical trapping potential $V(x)$. Then $C(x)$ can take positive or negative values, which divides the quantum wire into alternating regions of topological and trivial phases [Figs. 2(c) and 2(d)]. Exactly one MF mode localizes at each phase boundary. The position of the MFs can be changed by adiabatically moving a blue-detuned laser beam that changes $\mu(x)$. Similarly, we can also use focused Raman beams to induce spatially dependent $B(x)$ to control the positions of the MFs.

Floquet MFs.—It has been recently proposed that periodically driven systems can host nontrivial topological orders [19,20], which may even have unique behaviors with no analogue in static systems [21]. Our setup indeed allows one to turn a trivial phase topological by introducing time dependence, generating "Floquet MFs." For concreteness we consider the time-dependent chemical potential

$$\mu(t) = \begin{cases} \mu_1 & \text{for } t \in [nT, (n + 1/2)T) \\ \mu_2 & \text{for } t \in [(n + 1/2)T, (n + 1)T) \end{cases}, \qquad (3)$$

which can be implemented by varying the optical trap potential V or the rf frequency detuning $\delta_{\rm rf}$. In addition, we assume the presence of a 1D optical lattice. After unitary transformation U, the kinetic energy becomes spin-dependent $-2J\cos(pl+\sigma_z kl) = -2J\cos(kl)\cos(pl) + 2J\sin(kl)\sin(pl)\sigma_z$, where J is the tunnel matrix element and l is the lattice spacing. Hence, in Eq. (2) the spin-independent kinetic energy ε'_p is replaced by $-2J\cos(kl)\cos(pl)$ and the spin-orbit interaction $up\sigma_z$ is replaced by $2J\sin(kl)\sin(pl)\sigma_z$.

Let H_j be the Hamiltonian with $\mu = \mu_j$. The time-evolution operator after one period is then given by $U_T = e^{-iH_2T/2}e^{-iH_1T/2}$. We define an effective Hamiltonian from the relation $U_T \equiv e^{-iH_{\rm eff}T}$, and study the emergence of MFs in $H_{\rm eff}$. Eigenstates of $H_{\rm eff}$ are called Floquet states and represent stationary states of one period of evolution. The eigenvalues of $H_{\rm eff}$ are called quasienergies because they are only defined up to an integer multiple of $2\pi/T$. This feature, combined with the built-in particle-hole symmetry enjoyed by the Bogoliubov-de Gennes Hamiltonian, allows for Floquet MFs carrying *nonzero* quasienergy. That is, since states with quasienergy E and $-E$ are related by particle-hole symmetry, states with $E=0$ or $E=\pi/T \equiv -\pi/T$ can be their own particle-hole conjugates.

The existence of Floquet MFs is most easily revealed by plotting the quasienergy spectrum of $H_{\rm eff}$ in a finite system, which in practice can be created by introducing a confinement along the quantum wire. In Fig. 3, we plot the spectrum for a 100-site system with $\mu_1 = -J$, $\mu_2 = -3J$, $B = J$, $\Delta = 2J$, $2kl = \pi/4$ for varying drive period T. Note that both H_1 and H_2 correspond to the trivial phase with C_1, $C_2 > 0$. For small T, states with quasienergy $E=0$ or $E=\pi/T$ are clearly absent from the spectrum—i.e., there are no Floquet MFs here.

As one increases T, the gap at π/T closes, and for larger T a single Floquet state with $E=\pi/T$ remains. We have numerically checked that the amplitude for this Floquet state peaks near the ends of the 1D system. Thus it arises from two localized Floquet MFs and this state is associated with nontrivial topological charge Q_π as we will see below. As one further increases T, another state at quasienergy $E=0$ appears whose wave function again peaks near the two ends—a second type of Floquet MF—associated with a different, nontrivial topological charge Q_0. The two flavors of Floquet MFs at $E=0$ and $E=\pi/T$ are separated in quasienergies, and therefore, they are stable Floquet MFs as long as the periodicity of the drive is preserved. The presence of two particle-hole symmetric gaps changes the topological classification from Z_2 to $Z_2 \times Z_2$.

Two topological charges Q_0 and Q_π are defined as follows. For the translationally invariant quantum wire, the evolution operator has momentum decomposition $U_T(\tau) = \prod_p U_{T,p}(\tau)$ for intermediate time $\tau \in [0,T]$. After one evolution period, we have $U_T \equiv U_T(T)$ and $U_{T,p} \equiv U_{T,p}(T)$. The topological charge Q_0 (or Q_π) is the parity of the total number of times that the eigenvalues

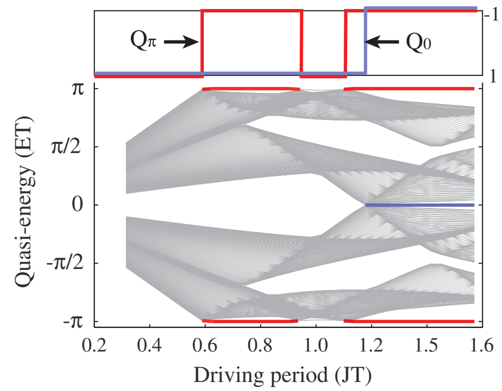

FIG. 3 (color online). Floquet MFs with two distinct flavors. Quasienergy spectrum of $H_{\rm eff}$ and topological charges (Q_0 and Q_π) are plotted for varying period T of the drive. Since the quasienergy is defined up to an integer multiple of $2\pi/T$, it can support Floquet MFs at $E=\pi/T$ (thick red [medium gray] line) as well as $E=0$ (thick blue [dark gray] line). The parameters are $\mu_1 = -J$, $\mu_2 = -3J$, $B=J$, $\Delta = 2J$, and $2ka = \pi/4$.

of $U_{T,0}(\tau)$ and $U_{T,\pi}(\tau)$ cross 1 (or -1). The topological charges have the closed form

$$Q_0 Q_\pi = {\rm Pf}[M_0]{\rm Pf}[M_\pi] \qquad Q_0 = {\rm Pf}[N_0]{\rm Pf}[N_\pi], \quad (4)$$

where $M_p = \log[U_{T,p}]$ and $N_p = \log[\sqrt{U_{T,p}}]$ are skew symmetric matrices associated with the evolution, and ${\rm Pf}[X]$ is the Pfaffian of matrix X. Here $\sqrt{U_{T,k}}$ is determined by the analytic continuation from the history of $U_{T,k}(\tau)$. Note that the product of topological charges Q_0Q_π is analogous to the Z_2 invariant suggested for static MFs [6]. In Fig. 3, we plot the topological charges Q_0 and Q_π for various driving period T. Indeed, Floquet states at $E=0$ and $E=\pi/T$ appear in the range of T at which Q_0 and Q_π equal to -1, respectively.

Probing MFs.—Radio-frequency spectroscopy can be used to probe MFs in cold-atom quantum wires [22,23]. In particular, we consider spatially resolved rf spectroscopy [24] as an analog of the STM. The idea is to use another probe rf field to induce a single particle excitation from the fermionic state (say a_σ) to an unoccupied fluorescent probe state f. Contrary to conventional rf spectroscopy, a tightly confined optical lattice strongly localizes the atomic state f, yielding a flat energy band for this state. By imaging the population in state f, we gain new spatial information about the local density of states.

For example, by applying a weak probe rf field with detuning $\delta'_{\rm rf}$ from the $a_\sigma - f$ transition, the population change in state f can be computed from the linear response theory $I(x,\nu) \equiv \frac{d}{dt}\langle f^\dagger(x)f(x)\rangle \propto \rho_{a_\sigma}[x, -\tilde{\mu}(x) - \delta'_{\rm rf} + \varepsilon]\Theta[\tilde{\mu}(x) + \delta'_{\rm rf} - \varepsilon]$. Since the MFs have zero energy in the band gap and are spatially localized at the end of the quantum wire, there will be an enhanced population transfer to state f with frequency $\delta'_{\rm rf} = \varepsilon - \mu(x^*)$ at the phase boundary x^*. If the $a_\sigma - f$ transition has good coherence, we can use a resonant rf π pulse to transfer the zero-energy population from a_σ to f, and then use ionization or *in situ* imaging techniques [25,26] to reliably readout the population in f with single particle resolution. Floquet MFs can also be detected in a similar fashion. Since a Floquet state at quasienergy E is the superposition of energy states with energies $E + 2n\pi/T$ for integer n, we should find the Floquet MFs at energies 0 (or π) $+2n\pi/T$ for 0 (or π) quasienergy Floquet MFs, respectively.

Parameters and imperfections.—We now estimate the experimental parameters for cold-atom quantum wires. (1) The spin-orbit interaction energy is $E_{\rm so} = mu^2/2 \leq E_{{\rm rec},0}$, with recoil energy $E_{\rm rec} \approx 30(2\pi)$ kHz for ^{6}Li atoms. If we use n sequential Λ transitions, the spin-orbit interaction strength can be increased to $u^{(n)} = nk/m$ and $E_{\rm so}^{(n)} = n^2 E_{\rm so}$. (2) The effective magnetic field $B = \frac{\Omega_1\Omega_2^*}{\delta_e}$ and the depth of the optical trap $V_0 \sim \frac{\Omega^2}{\delta}$ can be MHz, by choosing large detuning $\delta \sim 100(2\pi)$ THz and Rabi frequencies $\Omega \sim 50(2\pi)$ GHz, while still maintaining a low optical scattering rate $\Gamma \approx \frac{\Omega^2}{\delta^2}\gamma \sim 1(2\pi)$ Hz. (3) The transverse oscillation frequency of the 1D optical trap can be $\omega_\perp \approx \sqrt{\frac{4V_0}{mw^2}} \sim 150(2\pi)$ kHz for a laser beam with waist $w = 15$ μm. (4) The s-wave pairing energy $\Delta = g\Xi$ can be as large as $25(2\pi)$ kHz according to self-consistent calculation [27] assuming BEC density $n_0 = 10^{14}$ cm^{-3} [17], molecule scattering length 1 Å, and fermion transverse confinement $a_\perp = (\hbar/m\omega_\perp)^{1/2} \approx 0.1$ μm. When $\omega_\perp$ is much larger than $E_{\rm so}$ and $|\Delta|$, it is a good approximation to consider a single transverse mode.

In practice, there are various imperfections, such as particle losses, finite temperature of BEC, interaction among fermions, and multiple transverse modes of the quantum wire. (1) The lifetime associated with photon scattering induced loss can be improved to seconds using large detuning and strong laser intensity, and the collision-induced loss can be suppressed by adding a 1D optical lattice to the quantum wire. (2) The magnitude and phase fluctuations in the BEC order parameter can be efficiently suppressed by cooling the BEC well below the transition temperature. (3) Although the fermionic atoms may have positive scattering length, the tight transverse confinement can induce an effective attractive interaction for 1D fermionic atoms [28], which may further enhance the pairing energy. (4) Recent numerical and analytical studies [8,29,30] show that MFs can be robust even in the presence of multiple transverse modes, as long as an odd number of transverse channels are occupied.

In conclusion, we have proposed a scheme to create and probe MFs in cold-atom quantum wires, and suggested the creation of two nondegenerate flavors of Floquet MF at a single edge. We estimated the experimental parameters to realize such implementation, considered schemes to probe for MFs, and analyzed imperfections from realistic considerations. Recently, it has been discovered that braiding of non-Abelian anyons can be achieved in networks of 1D quantum wires [31], which would be very interesting to explore in the cold-atom context.

We would like to thank Ian Spielman for enlightening discussions. This work was supported by the Sherman Fairchild Foundation, DARPA OLE program, CUA, NSF, AFOSR Quantum Simulation MURI, AFOSR MURI on Ultracold Molecules, ARO-MURI on Atomtronics, and Dutch Science Foundation NWO/FOM.

[1] G. Moore and N. Read, Nucl. Phys. B **360**, 362 (1991).
[2] N. Read and D. Green, Phys. Rev. B **61**, 10 267 (2000).
[3] L. Fu and C. L. Kane, Phys. Rev. Lett. **100**, 096407 (2008).
[4] J. Linder *et al.*, Phys. Rev. Lett. **104**, 067001 (2010).
[5] J. D. Sau *et al.*, Phys. Rev. Lett. **104**, 040502 (2010); J. Alicea, Phys. Rev. B **81**, 125318 (2010); P. A. Lee, arXiv:0907.2681; S. Chung *et al.*, arXiv:1011.6422.
[6] A. Kitaev, Phys. Usp. **44**, 131 [2001].
[7] R. M. Lutchyn, J. D. Sau, and S. Das Sarma, Phys. Rev. Lett. **105**, 077001 (2010); Y. Oreg, G. Refael, and F. von Oppen, Phys. Rev. Lett. **105**, 177002 (2010).
[8] A. C. Potter and P. A. Lee, Phys. Rev. Lett. **105**, 227003 (2010); R. M. Lutchyn, T. D. Stanescu, and S. Das Sarma, Phys. Rev. Lett. **106**, 127001 (2011).
[9] Y. J. Lin *et al.*, Phys. Rev. Lett. **102**, 130401 (2009).
[10] Y. J. Lin *et al.*, Nature (London) **462**, 628 (2009); Y. J. Lin, K. JimenezGarcia, and I. B. Spielman, Nature (London) **471**, 83 (2011).
[11] J. Ruseckas *et al.*, Phys. Rev. Lett. **95**, 010404 (2005).
[12] K. Osterloh *et al.*, Phys. Rev. Lett. **95**, 010403 (2005).
[13] C. Zhang, Phys. Rev. A **82**, 021607 (2010).
[14] C. Zhang *et al.*, Phys. Rev. Lett. **101**, 160401 (2008).
[15] S. Zhu *et al.*, Phys. Rev. Lett. **106**, 100404 (2011).
[16] M. Sato, Y. Takahashi, and S. Fujimoto, Phys. Rev. Lett. **103**, 020401 (2009).
[17] M. Greiner, C. A. Regal, and D. S. Jin, Nature (London) **426**, 537 (2003); S. Jochim *et al.*, Science **302**, 2101 (2003); M. W. Zwierlein *et al.*, Phys. Rev. Lett. **91**, 250401 (2003).
[18] M. Holland *et al.*, Phys. Rev. Lett. **87**, 120406 (2001).
[19] T. Kitagawa *et al.*, Phys. Rev. A **82**, 033429 (2010).
[20] N. Lindner, G. Refael, and V. Galitski, Nature Phys. (to be published).
[21] T. Kitagawa *et al.*, Phys. Rev. B **82**, 235114 (2010).
[22] C. A. Regal and D. S. Jin, Phys. Rev. Lett. **90**, 230404 (2003); S. Gupta *et al.*, Science **300**, 1723 (2003); C. Chin *et al.*, Science **305**, 1128 (2004).
[23] S. Tewari *et al.*, Phys. Rev. Lett. **98**, 010506 (2007).
[24] L. Jiang *et al.*, arXiv:1010.3222.
[25] W. S. Bakr *et al.*, Nature (London) **462**, 74 (2009).
[26] J. F. Sherson *et al.*, Nature (London) **467**, 68 (2010).
[27] See supplemental material at http://link.aps.org/supplemental/10.1103/PhysRevLett.106.220402 for self-consistent calculation of pairing energy.
[28] M. Olshanii, Phys. Rev. Lett. **81**, 938 (1998).
[29] A. C. Potter and P. A. Lee, Phys. Rev. B **83**, 094525 (2011).
[30] M. Wimmer *et al.*, Phys. Rev. Lett. **105**, 046803 (2010).
[31] J. Alicea *et al.*, Nature Phys. **7**, 412 (2011).